



Volume 63B, No. 2, February 2008

ISSN 0584-8547

SPECTROCHIMICA ACTA

PART B: ATOMIC SPECTROSCOPY
Including Spectrochimica Acta Reviews

Spectrochimica Acta Part B
Editors
M.T.C. DE LOOS
Delft

N. OMENETTO
Gainesville, FL

Spectrochimica Acta Reviews
Editors
A. BOGAERTS
Wilrijk, Antwerp

J.-M. MERMET
Tromsø

R.E. STURGEON
Ottawa

HONORING ISSUE
A COLLECTION OF PAPERS ON ATOMIC,
MOLECULAR AND LASER SPECTROSCOPY

DEDICATED TO
JAMES D. WINEFORDNER

Available online at
ScienceDirect
www.sciencedirect.com

This article was published in an Elsevier journal. The attached copy is furnished to the author for non-commercial research and education use, including for instruction at the author's institution, sharing with colleagues and providing to institution administration.

Other uses, including reproduction and distribution, or selling or licensing copies, or posting to personal, institutional or third party websites are prohibited.

In most cases authors are permitted to post their version of the article (e.g. in Word or Tex form) to their personal website or institutional repository. Authors requiring further information regarding Elsevier's archiving and manuscript policies are encouraged to visit:

<http://www.elsevier.com/copyright>



Determination of the Rb atomic number density in dense rubidium vapors by absorption measurements of Rb₂ triplet bands [☆]

Vlasta Horvatic ^{a,*}, Damir Veza ^b, Kay Niemax ^c, Cedomil Vadla ^a

^a Institute of Physics, Bijenicka 46, 1000 Zagreb, Croatia

^b Department of Physics, Faculty of Science, University of Zagreb, Bijenicka 32, 10000 Zagreb, Croatia

^c ISAS, Institute for Analytical Sciences at the University of Dortmund, Bunsen-Kirchoff-Str. 11, D-44139, Dortmund, Germany

Received 2 October 2007; accepted 20 November 2007

Available online 4 December 2007

Abstract

A simple and accurate way of determining atom number densities in dense rubidium vapors is presented. The method relies on the experimental finding that the reduced absorption coefficients of the Rb triplet satellite bands between 740 nm and 750 nm and the triplet diffuse band between 600 nm and 610 nm are not temperature dependent in the range between 600 K and 800 K. Therefore, the absolute values of the reduced absorption coefficients of these molecular bands can provide accurate information about atomic number density of the vapor. The rubidium absorption spectrum was measured by spatially resolved white-light absorption in overheated rubidium vapor generated in a heat pipe oven. The absolute values for the reduced absorption coefficients of the triplet bands were determined at lower vapor densities, by using an accurate expression for the reduced absorption coefficient in the quasistatic wing of the Rb D1 line, and measured triplet satellite bands to the resonance wing optical depth ratio. These triplet satellite band data were used to calibrate in absolute scale the reduced absorption coefficients of the triplet diffuse band at higher temperatures. The obtained values for the reduced absorption coefficient of these Rb molecular features can be used for accurate determination of rubidium atomic number densities in the range from about $5 \times 10^{16} \text{ cm}^{-3}$ to $1 \times 10^{18} \text{ cm}^{-3}$.

© 2007 Elsevier B.V. All rights reserved.

Keywords: Rubidium; Infrared spectrum; Visible spectrum; Line intensities; Band intensities

1. Introduction

Since the early ages of spectroscopic investigations, alkalis have been subject of extensive investigations. Nowadays, they still attract considerable attention (Bose–Einstein condensates [1], long-range Rydberg molecules [2,3]). Numerous investigations involving alkali atoms are in great deal due to their simple structure which makes them relatively easy to deal with, experimentally as well as theoretically.

In the experiments performed with the aim to determine certain physical quantity or characterize the particular process,

[☆] This article is published in a special honor issue dedicated to Jim Winefordner on the occasion of his retirement, in recognition of his outstanding accomplishments in analytical atomic and molecular spectroscopy.

* Corresponding author. Tel.: +385 1 469 8861; fax: +385 1 469 8889.

E-mail address: blecic@ifs.hr (V. Horvatic).

knowledge about the number density of the medium is required in order to obtain quantitative results. It is always advantageous if the number density can be determined without knowing the temperature of the vapor. Namely, standard methods for number density determination, as vapor pressure curves [4], curve of growth [5–7], line peak absorption [8–14] or absorption in the impact resonance line wing [15–19], require the temperature to evaluate the density of the vapor. However, accurate measurements of the alkali vapor temperature are not always an easy task, unless the experiment is performed in a small glass cell placed in an oven with homogeneous temperature distribution. The method for obtaining atom number density straightforwardly, by the measurements of the absorption coefficient in the alkali quasistatic resonance wings [20] is advantageous in that regard, and it has been successfully used in many experiments so far [21–26]. However, this method is applicable at densities lower than $\approx 10^{17} \text{ cm}^{-3}$, because for the usual length of the

optical path of the order of 10 cm, the medium becomes opaque at the relevant wavelengths.

In the quest for the spectroscopic means of determination of the alkali number density at elevated pressures ($N > 10^{17} \text{ cm}^{-3}$), which would not involve determination of the vapor temperature, our attention was drawn to spectrally isolated molecular bands of alkali dimers which still appear optically thin at such high pressures. The semiclassical approach yields the following functional dependence of the absorption coefficient of a molecular band: $k \propto N^2 \times \exp[-\Delta V(R)/k_B T]$. Here, $\Delta V(R) = V(R) - V(\infty)$ is the difference potential for the lower dimer potential curve at the internuclear distance R . If the molecular bands are stemming from an interatomic range where the ground states are shallow ($\Delta V \ll k_B T$), the corresponding absorption coefficient will exhibit a weak dependence on temperature. In that case, the absorption coefficient depends on wavelength and can be expressed in the form $k(\lambda) = k_R(\lambda) \times N^2$, where k_R is the reduced absorption coefficient, which depends only on characteristic parameters of the particular molecular transition. The situation is analogous to the atomic absorption spectroscopy where $k = a \times N$, with a comprising the characteristic atomic spectral line parameters, i.e., oscillator line strengths. Therefore the k_R of such temperature insensitive molecular bands could serve as spectroscopic standard for straightforward (not involving temperature measurements) number density determination.

The alkali triplet transitions exhibit the described characteristics (see Fig. 1), and the results for the reduced absorption

coefficients of these bands, which can be used for a simple and accurate determination of the high atom number densities, have already been reported for potassium [27] and cesium [28].

An immediate motivation for this work came from the investigations dealing with experimental verification of minima in excited long-range Rydberg states of rubidium dimer [33]. The experiment was conducted in a dense Rb vapor ($p \approx 100 \text{ mbar}$), and accurate data on the Rb ground state number density were requisite for the evaluation of the results. The necessity of finding reliable spectroscopic means to determine rubidium ground state number density in such experimental conditions yielded the results which will be presented here.

2. Experiment and data analysis

2.1. Experimental details

The details of the present experiment were published previously [27–29] and will not be repeated here in length. The main task in setting-up the measurement was to create dense and stable rubidium vapor at pressure of about 100 mbar. This was accomplished by using a heat pipe with additional inner heater built-in along the heat pipe axis. The role of the inner heater was to prevent formation of turbulent fog of particle clouds at the hot–cold (alkali–buffer gas) boundaries and clogging in the cold zone. These processes are known to occur at alkali vapor pressures larger than a few tens of mbar, and can completely obstruct the measurements. An overheating realized

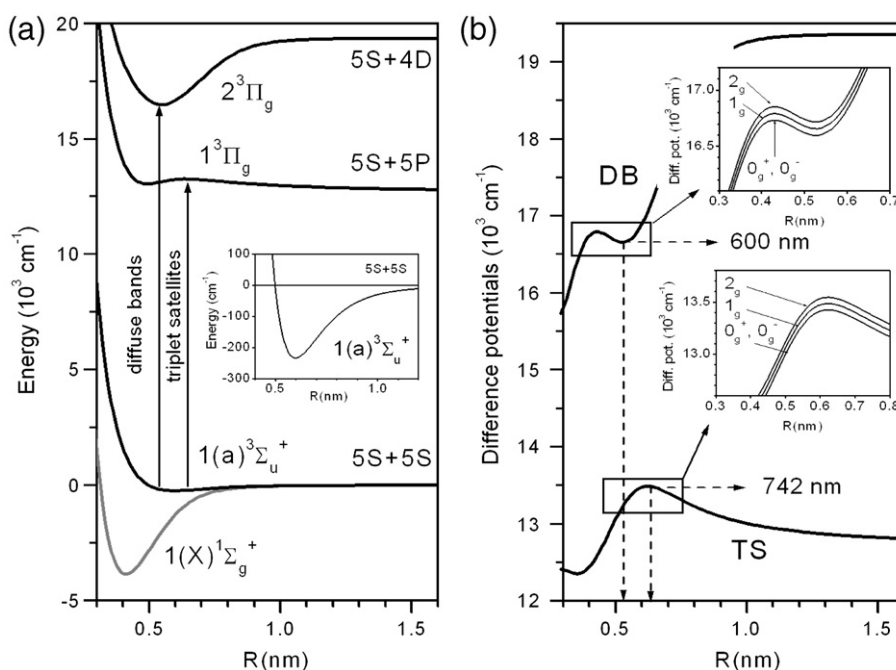


Fig. 1. (a) The triplet potentials $1(a)^3\Sigma_u^+$, $1^3\Pi_g$ [29], and $2^3\Pi_g$ [30] of Rb_2 involved in the formation of satellite and diffuse bands. The potentials shown are for Hund's case a (spin-orbit coupling not included). The relevant transitions are indicated with arrows. The singlet ground state $1(X)^1\Sigma_g^+$ involved in the formation of the singlet X-A and X-B bands is also shown. The inset shows enlarged view of the shallow (depth $\Delta V \approx 200 \text{ cm}^{-1}$) ground state triplet potential $1(a)^3\Sigma_u^+$. (b) The differential potentials for the $1(a)^3\Sigma_u^+ \rightarrow 1^3\Pi_g$ (triplet satellites — TS) and $1(a)^3\Sigma_u^+ \rightarrow 2^3\Pi_g$ (diffuse bands — DB) transitions (Hund's case a). The satellite and diffuse bands are due to the extrema in these potentials. The insets show the differential potentials for the transitions $1(a)^3\Sigma_u^+(1_u, 0_u) \rightarrow 1^3\Pi_g(0_g^+, 1_g, 2_g)$ [31] and $1(a)^3\Sigma_u^+(1_u, 0_u) \rightarrow 2^3\Pi_g(0_g^+, 1_g, 2_g)$ [32] in the Hund's case c (spin-orbit coupling included). Each single differential potential of the Hund's case a, now splits in three, and their maxima correspond to the observed three-peak structure of the Rb_2 triplet bands.

with the inner heater suppressed these processes and enabled production of spatially and temporally stable rubidium vapor. With built-in heater a radial temperature gradient was established across the rubidium vapor column, enabling measurements at different temperatures under the same steady state vapor conditions. The inner heater was so designed [28] to ensure that the temperature and consequently, the vapor number density distributions, were axially symmetric.

Concise technical information related to the instrumentation and experimental conditions is summarized in Table 1, while their detailed descriptions can be found in [27–29].

For the readers' convenience we reproduce here (Fig. 2a) the illustration of the measurement procedure. A collimated white-light beam of a halogen lamp was shown through the strongly overheated Rb vapor column with radial temperature and number density gradient. The transmitted light was imaged in 1:1 ratio onto a screen positioned at 3 cm distance from the monochromator entrance slit. The screen had a pinhole of 0.5 mm in diameter, and the transmitted intensity eventually falling onto the entrance slit was related to a thin column of about 0.5 mm in diameter, located at the position r from the heat pipe axis. The spatially resolved Rb spectra were obtained by translating the heat pipe radially in discrete steps, and measuring the optical depths $k(r, \lambda)L = \ln[I_0(\lambda)/I(r, \lambda)]$ in the zones at different radial positions r , having correspondingly different temperatures. The data were collected using LabView program and stored on a laboratory PC for subsequent analysis.

The representative spectra of spatially resolved absorption in rubidium vapor recorded in the way described above are shown in Fig. 2b. The main spectral features in the investigated spectral range are the rubidium resonance lines with extended quasi-static wings, overlapping with strongly temperature dependent Rb₂ singlet bands (X-A and X-B).

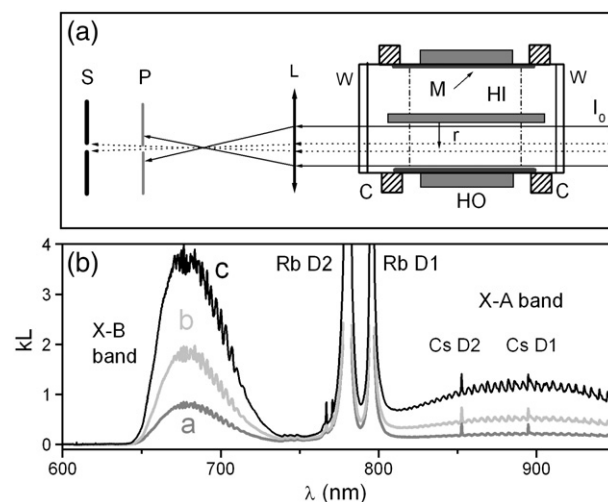


Fig. 2. (a) Experimental arrangement for the spatially resolved absorption measurements in overheated Rb vapor generated in the heat pipe. S — monochromator entrance slit, P — pinhole, L — lens, C — water cooling, W — windows, M — mesh with liquid rubidium, HO — outer heater, HI — inner heater, I_0 — incident collimated white-light beam. (b) Measured optical depths kL in overheated rubidium vapor at radial positions $r_a=3$ mm (near the inner heater, spectrum a), $r_b=6$ mm (spectrum b), and $r_c=9$ mm (near the heat pipe wall, spectrum c).

2.2. Determination of the Rb number density from the absorption in the Rb D1 resonance line wing

A detailed insight into the data plotted in Fig. 2b is given in Fig. 3, which shows the spectra in the vicinity of the Rb resonance lines for radial position near the inner heater (spectrum a) and near the heat pipe wall (spectrum c). The wings of the resonance lines are due to electronic transitions in the long-range region where the ground state interaction potentials are shallow and the corresponding Boltzmann factor nearly equals to unity at thermal conditions [20,29]. Therefore, the resonance line wings are practically insensitive to the temperature variation at the temperatures investigated in the present experiment.

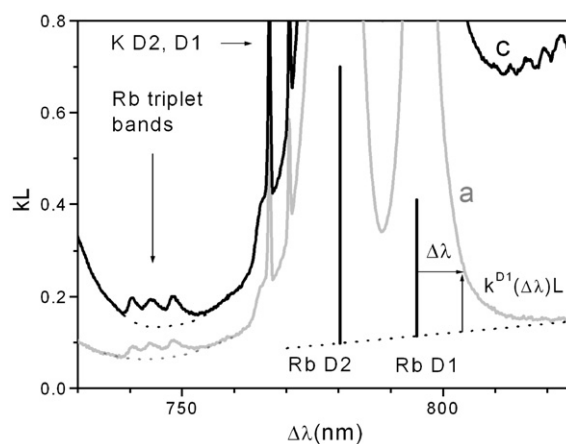


Fig. 3. The details of a and c spectra from Fig. 2, in the vicinity of the Rb first resonance doublet. The spectra were recorded at the distances $r_a=3$ mm and $r_c=9$ mm from the heat pipe axis. The estimated molecular backgrounds are depicted with dotted lines.

Table 1
Summary of the information about instrumentation and experimental conditions

Item	Description
Heat pipe	Stainless-steel with quartz windows and a stainless-steel mesh liner Inner diameter: 2 cm, windows distance: 18 cm Operating mode: heat pipe
Heat pipe heaters	Outer — resistance: 38 Ω, power: typically 150 W Inner — 250 μm thick Mo wire helix (diameter: 2 mm, length: 12 cm, resistance: 2 Ω), power: typically 10 W
Vapor column length	$L=6.5$ cm
Hot-cold boundary	Width: a few millimeters
Buffer gas	Ar
Monochromator	0.5 m Jarrel–Ash, spectral resolution: 0.1 nm
Photomultiplier	RCA 7102 photomultiplier (S-1 cathode) cooled down to -20 °C
Light source	Halogen lamp
Temperatures	At the heat pipe wall: $T_w \approx 650$ K At the edge of the inner heater: $T_A \approx 900$ K
Rb number densities	Between 5×10^{16} cm ⁻³ and 1×10^{18} cm ⁻³

As shown in Ref. [20], the blue quasistatic wings of D2 and the red wings of D1 alkali resonance lines can be used for accurate determination of atomic number density. In the first step of data analysis performed here, the red wing of the Rb D1 line was used for determination of the rubidium number density.

According to [20,25], the absorption coefficient k_{D1} (in cm^{-1}) in the red wing of the Rb D1 line at the detuning $\Delta\lambda$ (in nm) from the line center can be expressed as:

$$k_{D1}^{\text{red}}(\Delta\lambda) = 5.02 \times 10^{-34} P(\Delta\lambda/\Delta_{\text{fs}}) \frac{N^2}{(\Delta\lambda)^2}, \quad (1)$$

where the rubidium number density N is expressed in cm^{-3} , and Δ_{fs} is the fine structure splitting of the rubidium resonance doublet ($\Delta_{\text{fs}} = 14.78$ nm). The polynomial $P(\Delta\lambda/\Delta_{\text{fs}})$ defined by the following relation:

$$P(\Delta\lambda/\Delta_{\text{fs}}) = 1.0317 + 2.2934 \left(\frac{\Delta\lambda}{\Delta_{\text{fs}}}\right) - 0.6319 \left(\frac{\Delta\lambda}{\Delta_{\text{fs}}}\right)^2 + 0.0732 \left(\frac{\Delta\lambda}{\Delta_{\text{fs}}}\right)^3 \quad (2)$$

represents the fit to the theoretical wing profile. The fit reproduces the numerical theoretical profile with an accuracy better than ± 0.5 for the values of $\Delta\lambda$ in the range $1 \text{ nm} \leq \Delta\lambda \leq 3\Delta_{\text{fs}}$. Consequently, Eq. (1) is valid and applicable in the same range of detunings $\Delta\lambda$ in the line wing.

In contrast to the resonance line wings, the absorption coefficients of both X-A and X-B molecular bands are strongly temperature dependent, because the corresponding Boltzmann factors are very sensitive to temperature in the investigated temperature range. The resonance lines are superimposed on the red tail of the X-A band. The contribution of the latter to the total optical depth in the vicinity of the resonance lines can be approximated by a straight line as illustrated in Fig. 3. The height and slope of the straight line representing molecular background, which was subtracted from the measured data, was determined by varying the straight line fit parameters until the remaining optical depth $k^{\text{D1}}(\Delta\lambda)L$ exhibited the wavelength dependence defined by Eq. (1). Using this corrected $k^{\text{D1}}(\Delta\lambda)L$ values and the estimated vapor column length $L = (6.5 \pm 0.5)$ cm, from Eq. (1) one obtains the value for the rubidium number density $N(r)$ at a given distance r from the heat pipe axis with an accuracy of about 3%, which is mainly due to the vapor column length uncertainty. For the spectra plotted in Figs. 2 and 3, this evaluation method yielded the values $N(r_a) = 4.25 \times 10^{16} \text{ cm}^{-3}$, $N(r_b) = 4.66 \times 10^{16} \text{ cm}^{-3}$, and $N(r_c) = 5.05 \times 10^{16} \text{ cm}^{-3}$, at the positions $r_a = 3$ mm, $r_b = 6$ mm and $r_c = 9$ mm, respectively.

2.3. Determination of the temperature distribution

The Rb atom number density $N(r_w)$ just above the liquid metal bath in the mesh on the heat pipe wall ($r_w = 10$ mm) was obtained by extrapolation of the $N(r_a)$, $N(r_b)$ and $N(r_c)$ values. The vapor in the immediate vicinity of the mesh is in thermal equilibrium with liquid metal bath. Therefore, it is justified to determine the corresponding vapor temperature T_w near the heat pipe wall by using the $N(r_w)$, rubidium vapor pressure curve [4]

and the ideal gas law. Because the rubidium in the heat pipe constantly re-circulates through the mesh, the metal vapor column is in dynamical equilibrium and the vapor pressure is equal throughout the heat pipe volume. Therefore, by using ideal gas law, the temperature at the particular distance r from the heat pipe axis can be determined from the following relation:

$$T(r) = T(r_w) \frac{N(r_w)}{N(r)}. \quad (3)$$

It should be emphasized that in the conditions of the present experiment the density of rubidium dimers is negligible in comparison with the atomic number density [4]. In the case presented in Figs. 2 and 3, the obtained values for the temperatures $T(r_a)$, $T(r_b)$, $T(r_c)$ were 745 K, 675 K and 625 K. The accuracy of these data is about 6%. The declared error bar comprises the inaccuracy in the atom number density determination, extrapolation procedure yielding $N(r_w)$ value and uncertainty in the Rb vapor pressure curve.

3. Triplet satellites between 740 and 750 nm

The rubidium triplet satellites at the wavelengths between 740 and 750 nm become measurable in absorption at vapor densities where the resonance line wings can still be reliably analyzed. Owing to this fact, the optical depths of the triplet satellites $\tau^{\text{TS}}(\lambda) = k^{\text{TS}}(\lambda)L$ could be directly compared to the optical depth $\tau_{D1}^{\text{red}}(\Delta\lambda) = k_{D1}^{\text{red}}(\Delta\lambda)L$ of the resonance wing at a given detuning $\Delta\lambda$. By substituting the ratio of the measured optical depths into Eq. (1), the reduced absorption coefficient $k_{\text{R}}^{\text{TS}} = k^{\text{TS}}(\lambda)/N^2$ could be accurately determined (in units cm^5) according to the following relation:

$$k_{\text{R}}^{\text{TS}}(\lambda) = \frac{\tau^{\text{TS}}(\lambda)}{\tau_{D1}^{\text{red}}(\Delta\lambda)} \times 5.02 \times 10^{-34} \times \frac{P(\Delta\lambda/\Delta_{\text{fs}})}{(\Delta\lambda)^2}. \quad (4)$$

The determination of the reduced absorption coefficient in this way did not require knowledge of rubidium number density and it canceled the contribution to the error bar from the uncertainty of the vapor column length L . However, to examine the temperature behavior of the investigated triplet satellite bands, the atom number densities had to be determined eventually, in order to evaluate the temperature of the vapor in the manner described in the previous section.

The total reduced absorption coefficient in the vicinity of the triplet satellites, obtained by comparison with the absorption in the red wing of the Rb D1 line is displayed in Fig. 4. The investigated triplet band lies on a background formed by the contributions arising from the red tail of the X-B band, the blue tail of X-A band and the far red wing of the resonance doublet. This background is continuous and it can be easily subtracted from the total reduced absorption coefficient in the region of the triplet band, as indicated by dashed line in Fig. 4. As can be seen in the inset of Fig. 4, the remaining contributions, i.e. the values for the reduced absorption coefficients $k_{\text{R}}^{\text{TS}}(\lambda)$ obtained at $T_a = 745$ K and $T_c = 625$ K are independent of temperature within the experimental error bar. Averaged values of the measurements

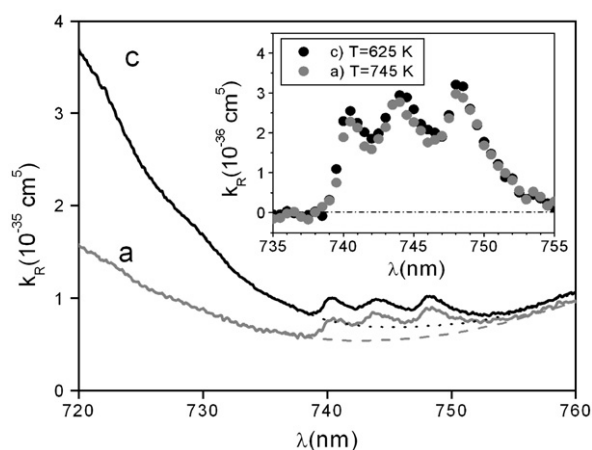


Fig. 4. The reduced absorption coefficient in the vicinity of the rubidium triplet satellites, obtained by comparison with the absorption in the red wing of the Rb D1 line. The experimental conditions were the same as for the data shown in Figs. 2 and 3. The estimated backgrounds are indicated with dashed and dotted lines. The inset shows the reduced absorption coefficient of the triplet satellite bands measured at $T_a=745$ K (gray dots) and $T_c=625$ K (black dots).

at several temperatures of the triplet satellite peaks at the wavelengths 740.5, 744.2 and 748.2 nm are:

$$k_R^{TS}(740.5) = (2.2 \pm 0.2) \times 10^{-36} \text{ cm}^5 \quad (5)$$

$$k_R^{TS}(744.2) = (2.8 \pm 0.3) \times 10^{-36} \text{ cm}^5 \quad (6)$$

$$k_R^{TS}(748.2) = (3.0 \pm 0.3) \times 10^{-36} \text{ cm}^5. \quad (7)$$

Numerical values of the $k_R^{TS}(\lambda)$ in the wavelength region between 738 nm and 755.4 nm are listed in Table 2. They are obtained as an average of several measurements at different temperatures.

4. Diffuse band between 600 and 610 nm

At elevated vapor densities (N about 10^{17} cm^{-3}) the rubidium diffuse band, situated between 600 and 610 nm, exhibiting three pronounced peaks at 601.3, 603.7 and 606.2 nm, becomes measurable. At such high pressures, the total absorption occurred in the region of X-A and X-B bands, as well as in the wavelength range of the resonance lines. Therefore, the latter could no more be used for the number density diagnostic. However, the absorption was still reliably measurable at the triplet satellite band (see Fig. 5), and the Rb number density could be determined by using Eqs. (5)–(7) and the measured value of the corresponding absorption coefficient.

According to the theoretical results published in Ref. [29], the tail of the X-B band vanishes at about 630 nm, and there are no other molecular contributions to the absorption in the wavelength interval of the diffuse band. However, as can be seen in Fig. 5, the measurements show that the diffuse band lies on a weak continuum, which does not depend on temperature and increases proportionally to N^2 . Similarly to the case of potassium [27], it is assumed that this flat continuum is a consequence of alkali clusters formed in the region of hot–cold

Table 2

The reduced absorption coefficient of the rubidium triplet satellite band (in units 10^{-36} cm^5) in dependence on the wavelength

λ (nm)	k_R^{TS}						
738	0.011	743	2.242	748	2.904	753	0.506
738.2	0.019	743.2	2.413	748.2	2.967	753.2	0.459
738.4	0.058	743.4	2.579	748.4	2.936	753.4	0.422
738.6	0.113	743.6	2.702	748.6	2.846	753.6	0.394
738.8	0.259	743.8	2.765	748.8	2.723	753.8	0.353
739	0.421	744	2.795	749	2.574	754	0.327
739.2	0.629	744.2	2.77	749.2	2.403	754.2	0.318
739.4	0.921	744.4	2.713	749.4	2.232	754.4	0.281
739.6	1.258	744.6	2.631	749.6	2.079	754.6	0.246
739.8	1.565	744.8	2.541	749.8	1.934	754.8	0.211
740	1.853	745	2.446	750	1.798	755	0.18
740.2	2.092	745.2	2.345	750.2	1.655	755.2	0.151
740.4	2.214	745.4	2.231	750.4	1.521	755.4	0.139
740.6	2.243	745.6	2.122	750.6	1.398		
740.8	2.222	745.8	2.009	750.8	1.294		
741	2.146	746	1.944	751	1.207		
741.2	2.052	746.2	1.881	751.2	1.109		
741.4	1.977	746.4	1.839	751.4	1.013		
741.6	1.893	746.6	1.839	751.6	0.926		
741.8	1.815	746.8	1.889	751.8	0.846		
742	1.795	747	1.985	752	0.759		
742.2	1.817	747.2	2.136	752.2	0.684		
742.4	1.848	747.4	2.353	752.4	0.646		
742.6	1.953	747.6	2.561	752.6	0.603		
742.8	2.091	747.8	2.749	752.8	0.553		

boundary in the heat pipe, which act as a kind of neutral density filter.

By using the triplet satellite band as the temperature insensitive standard for the rubidium number density determination, the vapor temperature distribution was determined in the same manner as described in Section 2.3. The reduced absorption coefficient $k_R^{DB}(\lambda)$ of the diffuse band was evaluated by measuring the optical depth of the diffuse band

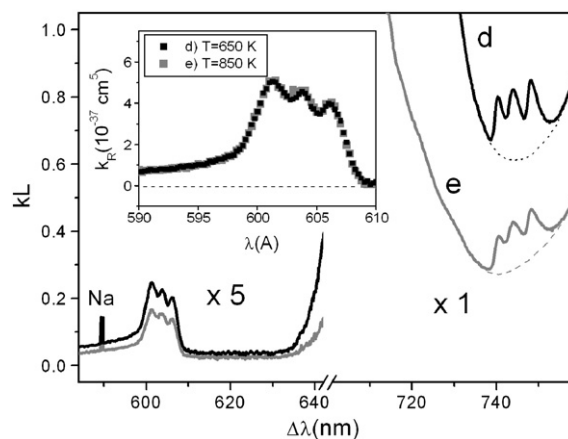


Fig. 5. Absorption spectrum of the rubidium diffuse band shown together with the sequence in the region of the triplet satellite band. The spectra were recorded at two positions: near the heat pipe wall (label d) and near the inner heater (label e). The rubidium number density and the vapor temperature for were: d-spectrum, $N_d=1.1 \times 10^{17} \text{ cm}^{-3}$ and $T_d=650$ K; e-spectrum, $N_e=8.7 \times 10^{16} \text{ cm}^{-3}$ and $T_e=800$ K. The inset shows the reduced absorption coefficient of the rubidium diffuse band for the two investigated temperatures.

Table 3

The reduced absorption coefficient of the rubidium diffuse band (in units 10^{-37} cm^5). The data are related to the flat absorption continuum at 620 nm (see text for further explanations)

λ (nm)	k_{R}^{DB}						
590	0.7	595	0.99	600	3.585	605	3.451
590.2	0.709	595.2	1.006	600.2	3.813	605.2	3.442
590.4	0.719	595.4	1.024	600.4	4.047	605.4	3.489
590.6	0.73	595.6	1.081	600.6	4.404	605.6	3.665
590.8	0.7386	595.8	1.087	600.8	4.603	605.8	3.788
591	0.733	596	1.097	601	4.923	606	3.862
591.2	0.763	596.2	1.179	601.2	5.005	606.2	3.889
591.4	0.752	596.4	1.202	601.4	4.997	606.4	3.774
591.6	0.766	596.6	1.219	601.6	4.893	606.6	3.617
591.8	0.786	596.8	1.271	601.8	4.728	606.8	3.348
592	0.803	597	1.282	602	4.661	607	3.069
592.2	0.795	597.2	1.331	602.2	4.43	607.2	2.695
592.4	0.81	597.4	1.362	602.4	4.316	607.4	2.222
592.6	0.822	597.6	1.415	602.6	4.201	607.6	1.883
592.8	0.83	597.8	1.448	602.8	4.149	607.8	1.569
593	0.846	598	1.512	603	4.237	608	1.404
593.2	0.854	598.2	1.597	603.2	4.336	608.2	1.184
593.4	0.894	598.4	1.654	603.4	4.395	608.4	0.978
593.6	0.902	598.6	1.799	603.6	4.437	608.6	0.767
593.8	0.9	598.8	1.958	603.8	4.457	608.8	0.599
594	0.91	599	2.113	604	4.369	609	0.492
594.2	0.939	599.2	2.52	604.2	4.185	609.2	0.393
594.4	0.975	599.4	2.783	604.4	3.984	609.4	0.304
594.6	0.973	599.6	3.099	604.6	3.737	609.6	0.248
594.8	0.997	599.8	3.325	604.8	3.624	609.8	0.225

($\tau^{\text{DB}}(\lambda) = k^{\text{DB}}(\lambda)L$) relative to the optical depth $\tau^{\text{TS}}(\lambda)$ of the triplet satellite. In this manner, the error introduced by the uncertainty in the value of the optical path L canceled out, similarly as in the case of calibration of the intensity of the triplet satellites by the intensity of the resonance wing. In the evaluation of the optical depth $\tau^{\text{DB}}(\lambda)$ the height of the flat continuum at 620 nm was subtracted. The analysis showed (see inset of Fig. 5) that the reduced absorption coefficient of the diffuse band, alike the triplet satellite, exhibited no temperature dependence in the investigated temperature interval. The values of the reduced absorption coefficients for the three peaks of the diffuse band at wavelengths of 601.3, 603.7 and 606.2 nm were obtained by taking the average of several measurements, and they read:

$$k_{\text{R}}^{\text{DB}}(601.3) = (5.0 \pm 0.7) \times 10^{-37} \text{ cm}^5 \quad (8)$$

$$k_{\text{R}}^{\text{DB}}(603.7) = (4.5 \pm 0.7) \times 10^{-37} \text{ cm}^5 \quad (9)$$

$$k_{\text{R}}^{\text{DB}}(606.2) = (3.9 \pm 0.7) \times 10^{-37} \text{ cm}^5. \quad (10)$$

The declared error bar includes the uncertainty of the reduced absorption coefficient of the triplet satellites used in the evaluation of the results.

The numerical values of the $k_{\text{R}}^{\text{DB}}(\lambda)$ in the region between 590 nm and 610 nm, obtained by averaging several measurements at different temperatures in the investigated range are given in Table 3.

5. Discussion and conclusion

Rubidium triplet bands in the visible region have been subject of many investigations in the past (see for instance [31,32] and references therein). The primary motivation was examination of the structure and dynamics of Rb_2 dimer at various internuclear separations. The experimental data of the triplet satellite and diffuse rubidium bands that are available in literature so far, concern only their relative intensity (in arbitrary units). In the present work, absolute values of their reduced absorption coefficients have been reported for the first time.

For the possible application of these reduced absorption coefficients as spectroscopic standards for the Rb number density determination in the conditions of dense vapors, it was important to examine whether they are sensitive to temperature variations. To accomplish this, the spatially resolved measurements were performed in overheated rubidium vapor. It was found out that the reduced absorption coefficients of both the satellite and diffuse bands, do not depend on temperature in the range from 625 to 800 K. In other words the absorption coefficients $k^{\text{TS}}(\lambda)$ and $k^{\text{DB}}(\lambda)$ are solely the functions of N^2 .

The triplet satellite bands between 740 nm and 750 nm are due the transitions (see Fig. 1) from the Rb_2 $^3\Sigma_u^+$ (asymptote: $5S+5S$) ground state to the $^3\Pi_g$ (asymptote: $5S+5P$) state [31]. These transitions occur in the narrow range of internuclear distances at about 0.6 nm due to extrema in the differential potential curves (Hund's case c: ground state potentials $0_u^-, 1_u$, excited state potentials $0_g^+, 0_g^-, 1_g, 2_g$). According to theory [29], the corresponding $\Delta V \approx 200 \text{ cm}^{-1}$, which means that the theoretical value of the Boltzmann factor $\exp[-\Delta V/k_B T]$ varies about 5% in the investigated temperature range ($T=700 \pm 100$). Similar estimation is also obtained for the diffuse band occurring in the $^3\Sigma_u^+ (5S+5S) \rightarrow ^3\Pi_g (5S+4D)$ transition. These assessments show that the variations of these molecular features with temperature are within the experimental error bars of the presented data and could not be discriminated in the present experiment.

An estimate of the upper limit of the temperature interval in which the rubidium diffuse band can be used for the number density determination is illustrated by the following example. With the optical depth being $k(\lambda)L=3$ (absorption of about 95%) at the wavelength of the weakest peak ($\lambda=606.2 \text{ nm}$, $k_{\text{R}}(\lambda) = k(\lambda)/N^2 = 3.9 \times 10^{-37} \text{ cm}^5$) and the optical path $L=6.5 \text{ cm}$, one obtains $N=(1.10 \pm 0.03) \times 10^{18} \text{ cm}^{-3}$. The temperature which, according to the equilibrium vapor pressure curve [4], corresponds to this number density, is $T \approx 800 \text{ K}$. This temperature just coincides with the upper boundary of the temperature interval within which the theoretically predicted temperature variation of the reduced absorption coefficient would still be smaller than the experimental error bar in the present investigation.

We may conclude that the investigations of the rubidium triplet satellite band (between 740 and 750 nm) and the diffuse band (between 600 and 610 nm) band were made in order to investigate whether they are reliable standards for the spectroscopic determination of the Rb number densities in a dense vapor. The measurements were performed in an overheated Rb vapor created in a heat pipe, and the mentioned spectral features were investigated by spatially resolved white-light absorption.

The method enabled measurements in the range of Rb densities between $5 \times 10^{16} \text{ cm}^{-3}$ and $1 \times 10^{18} \text{ cm}^{-3}$, and at temperatures in the range from 600 to 800 K. It has been experimentally verified that the reduced absorption coefficients of the rubidium triplet satellite and diffuse bands are, within the experimental error bar, independent of temperature in the investigated temperature range. Consequently, they can be used as reliable spectroscopic standards for the Rb number density determination at elevated pressures.

Acknowledgement

The presented results were obtained within the frame of the project No. 035-0352851-2853 realized with the financial support of the Ministry of Science, Education and Sports of the Republic of Croatia. Funding by the Deutsche Forschungsgemeinschaft (DFG, project 436KRO113/9) is gratefully acknowledged. The authors also thank the Ministry of Innovation, Science, Research and Technology of the state North Rhine-Westphalia and the Ministry of Education and Research of the Federal Republic of Germany for general support.

References

- [1] J. Weiner, V.S. Bagnato, S. Zilio, P.S. Julienne, Experiments and theory in cold and ultracold collisions, *Rev. Mod. Phys.* 71 (1999) 1–85.
- [2] A.L. de Oliveira, M.W. Mancini, V.S. Bagnato, L.G. Marcassa, Rydberg cold collisions dominated by ultralong range potential, *Phys. Rev. Lett.* 90 (2003) 143002(1)–143002(4).
- [3] S.M. Farooqi, D. Tong, S. Krishnan, J. Stanojevic, Y.P. Zhang, J.R. Ensher, A.S. Estrin, C. Boisseau, R. Côté, E.E. Eyler, P.L. Gould, Long-range molecular resonances in a cold Rydberg gas, *Phys. Rev. Lett.* 91 (2003) 183002(1)–183002(4).
- [4] A.N. Nesmeyanov, *Vapor Pressure of the Chemical Elements*, Elsevier, London, 1963.
- [5] A. Thorne, U. Litzén, S. Johanson, *Spectrophysics — Principles and Applications*, Springer Verlag, Berlin–New York–Tokio, 1999.
- [6] C. Vadla, V. Horvatic, K. Niemax, Oscillator strength of the strongly forbidden $\text{Pb } 6p^2 \ ^3\text{P}_0 \rightarrow 6p^2 \ ^3\text{P}_1$ transition at 1278.9 nm, *Eur. Phys. J. D.* 14 (2001) 23–25.
- [7] J. Franzke, H.D. Wizemann, K. Niemax, C. Vadla, Impact broadening and shift rates for the $6p^2 \ ^3\text{P}_J \rightarrow 7s \ ^3\text{P}_J^0$ transitions of lead induced by collisions with argon and helium, *Eur. Phys. J. D.* 8 (2000) 23–28.
- [8] C. Vadla, K. Niemax, V. Horvatic, R. Beuc, Population and deactivation of lowest lying barium levels by collisions with He, Ar, Xe and Ba ground state atoms, *Z. Phys. D.* 34 (1995) 171–184.
- [9] C. Vadla, V. Horvatic, The $6s5d \ ^1\text{D}_2 \rightarrow 6s5d \ ^3\text{D}_J$ excitation energy transfer in barium induced by collisions with He, Ar and Xe atoms, *FIZIKA A* 4 (1995) 463–472.
- [10] C. Vadla, Energy pooling in caesium vapour: $\text{Cs}^*(6P_J) + \text{Cs}^*(6P_J) \rightarrow \text{Cs}(6S) + \text{Cs}^*(6D)$ *Eur. Phys. J. D.* 1 (1998) 259–264.
- [11] C. Vadla, K. Niemax, V. Horvatic, Energy pooling to the $\text{Ba } 6s6p \ ^1\text{P}_1^0$ level arising from collisions between pairs of metastable $\text{Ba } 6s5d \ ^3\text{D}_J$ atoms, *Eur. Phys. J., D* 1 (1998) 139–147.
- [12] M. Movre, V. Horvatic, C. Vadla, Caesium 6P fine-structure mixing and quenching induced by collisions with ground-state caesium atoms and molecules, *J. Phys. B* 32 (1999) 4647–4666.
- [13] M. Movre, C. Vadla, V. Horvatic, Mixing and quenching of the $\text{Cs } 5D_J$ states induced by collisions with caesium ground-state atoms, *J. Phys. B* 33 (2000) 3001–3012.
- [14] V. Horvatic, T.L. Correll, N. Omenetto, C. Vadla, J.D. Winefordner, The effects of saturation and velocity selective population in two-step $6S_{1/2} \rightarrow 6P_{3/2} \rightarrow 6D_{5/2}$ laser excitation in cesium, *Spectrochim. Acta Part B* 61 (2006) 1260–1269.
- [15] V. Horvatic, C. Vadla, M. Movre, The collision cross sections for excitation energy transfer in $\text{Rb}^*(5P_{3/2}) \text{K}(4S_{1/2}) \rightarrow \text{Rb}^*(5S_{1/2}) + \text{K}^*(4P_J)$ processes, *Z. Phys. D* 27 (1993) 123–130.
- [16] V. Horvatic, D. Veza, M. Movre, K. Niemax, C. Vadla, Collision cross sections for excitation energy transfer in $\text{Na}^*(3P_{1/2}) + \text{K}(4S_{1/2}) \leftrightarrow \text{Na}^*(3P_{3/2}) + \text{K}(4S_{1/2})$ processes, *Z. Phys. D* 34 (1995) 163–170.
- [17] V. Horvatic, C. Vadla, M. Movre, K. Niemax, The collision cross sections for the fine-structure mixing of caesium 6P levels induced by collisions with potassium atoms, *Z. Phys. D* 36 (1996) 101–104.
- [18] Correll, V. Horvatic, N. Omenetto, C. Vadla, J.D. Winefordner, Quantum efficiency improvement of a cesium based resonance fluorescence detector by helium-induced collisional excitation energy transfer, *Spectrochim. Acta Part B* 60 (2005) 765–774.
- [19] T.L. Correll, V. Horvatic, N. Omenetto, J.D. Winefordner, C. Vadla, Experimental evaluation of the cross sections for the $\text{Cs}(6D) \rightarrow \text{Cs}(7P_J)$ and $\text{Cs}(6D_{5/2}) \rightarrow \text{Cs}(6D_{3/2})$ collisional transfer processes induced by He and Ar, *Spectrochim. Acta Part B* 61 (2006) 623–633.
- [20] V. Horvatic, R. Beuc, M. Movre, C. Vadla, The non-Lorentzian wings of alkali resonance lines: the determination of the number density in pure and mixed alkali vapours, *J. Phys. B: At. Mol. Opt. Phys.* 26 (1993) 3679–3692.
- [21] C. Vadla, M. Movre, V. Horvatic, Sodium 3P fine-structure excitation transfer induced by collisions with rubidium and caesium atoms, *J. Phys. B: At. Mol. Opt. Phys.* 27 (1994) 4611–4622.
- [22] V. Horvatic, C. Vadla, M. Movre, K. Niemax, The collision cross sections for the fine-structure mixing of caesium 6P levels induced by collisions with potassium atoms, *Z. Phys. D* 36 (1996) 101–104.
- [23] C. Vadla, K. Niemax, J. Brust, Energy pooling in cesium vapor, *Z. Phys. D* 37 (1996) 241–247.
- [24] V. Horvatic, M. Movre, C. Vadla, Cross sections for the $\text{Na}(4D) \rightarrow \text{Na}(4F)$ excitation energy transfer induced by collisions with He, Ar and Na atoms, *J. Phys. B* 30 (1997) 4943–4954.
- [25] V. Horvatic, M. Movre, C. Vadla, The temperature dependence of the cross section for the energy pooling process $\text{Na}(3P) + \text{Na}(3P) \rightarrow \text{Na}(4D) + \text{Na}(3S)$, *J. Phys. B: At. Mol. Opt. Phys.* 32 (1999) 4957–4976.
- [26] V. Horvatic, Temperature dependence of the cross section σ_{ss} for the energy pooling process $\text{Na}(3P_0) + \text{Na}(3P) \rightarrow \text{Na}(5S) + \text{Na}(3S)$, *FIZIKA A* 12 (2003) 97–114.
- [27] C. Vadla, R. Beuc, V. Horvatic, M. Movre, A. Quentmeier, K. Niemax, Comparison of theoretical and experimental red and near infrared absorption spectra in overheated potassium vapor, *Eur. Phys. J. D* 37 (2006) 37–49.
- [28] C. Vadla, V. Horvatic, K. Niemax, Accurate determination of atomic number density in dense Cs vapors by absorption measurements of Cs_2 triplet bands, *Appl. Phys. B* 84 (2006) 523–527.
- [29] Beuc, M. Movre, V. Horvatic, C. Vadla, O. Dulieu, M. Aymar, Absorption spectroscopy of the rubidium dimer in an overheated vapor: an accurate check of molecular structure and dynamics, *Phys. Rev. A* 75 (2007) 032512(1)–032512(10).
- [30] O. Dulieu, private communication.
- [31] M.-L. Almazor, O. Dulieu, F. Masnou-Seeuws, R. Beuc, G. Pichler, Formation of ultracold molecules via photoassociation with blue detuned laser light, *Eur. Phys. J. D* 15 (2001) 355–363.
- [32] T. Ban, D. Aumiller, R. Beuc, G. Pichler, Rb_2 diffuse band emission excited by diode lasers, *Eur. Phys. D* 30 (2004) 57–64.
- [33] Greene, Hamilton, Crowell, Vadla, K. Niemax, Experimental verification of minima in excited long-range Rydberg states of Rb_2 , *Phys. Rev. Lett.* 97 (2006) 233002(1)–233002(4).